Author Manuscript

Author Manuscript

Author Manuscript

Author Manuscript

HHS Public Access

Author manuscript

Free Radic Biol Med. Author manuscript; available in PMC 2024 August 01.

Published in final edited form as:

Free Radic Biol Med. 2023 August 01; 204: 108–117. doi:10.1016/j.freeradbiomed.2023.04.023.

Pharmacological Ascorbate Induces Sustained Mitochondrial Dysfunction

Rory S. Carroll[1], **Juan Du**[1,2], **Brianne R. O'Leary**[1,2], **Garett Steers**[1], **Prabhat C. Goswami**[2,3,4], **Garry R. Buettner**[2,3,4], **Joseph J. Cullen**[1,2,3,4]

[1]Department of Surgery, University of Iowa College of Medicine.

[2]Department of Free Radical and Radiation Biology Program, University of Iowa College of Medicine.

[3]Department of Radiation Oncology, University of Iowa College of Medicine.

[4]Department of Holden Comprehensive Cancer Center, University of Iowa College of Medicine.

Abstract

Pharmacological ascorbate (P-AscH$^-$; high dose given intravenously) generates H_2O_2 that is selectively cytotoxic to cancer compared to normal cells. The RAS-RAF-ERK1/2 is a major signaling pathway in cancers carrying *RAS* mutations and is known to be activated by H_2O_2. Activated ERK1/2 also phosphorylates the GTPase dynamin-related protein (Drp1), which then stimulates mitochondrial fission. Although early generation of H_2O_2 leads to cytotoxicity of cancer cells, we hypothesized that sustained increases in H_2O_2 activate ERK-Drp1 signaling, leading to an adaptive response; inhibition of this pathway would enhance the toxicity of P-AscH$^-$. Increases in phosphorylated ERK and Drp1 induced by P-AscH$^-$ were reversed with genetic and pharmacological inhibitors of ERK and Drp1, as well as in cells lacking functional mitochondria. P-AscH$^-$ increased Drp1 colocalization to mitochondria, decreased mitochondrial volume, increased disconnected components, and decreased mitochondrial length, suggesting an increase in

Corresponding Author: Joseph J. Cullen, M.D., 1528 JCP, University of Iowa Hospitals and Clinics, Iowa City, IA 52242, joseph-cullen@uiowa.edu, telephone: (319) 353-8297.

Declaration of interests

The authors declare that they have no known competing financial interests or personal relationships that could have appeared to influence the work reported in this paper.

CRediT author statement

Rory S. Carroll: Conceptualization, formal analysis, validation, investigation, visualization, methodology, writing–original draft.
Juan Du: Formal analysis, validation, investigation, methodology.
Brianne R. O'Leary: Formal analysis, validation, investigation, visualization, methodology, writing–original draft, writing–review and editing.
Garett Steers: Formal analysis, investigation, methodology.
Prabhat C. Goswami: Conceptualization, supervision, methodology, writing–review and editing.
Garry R. Buettner: Writing–review and editing.
Joseph J. Cullen: Conceptualization, resources, supervision, funding acquisition, methodology, writing–original draft, project administration, writing–review and editing.

Conflict of Interest: The authors declare that they have no conflicts of interest with the contents of this article.

Publisher's Disclaimer: This is a PDF file of an unedited manuscript that has been accepted for publication. As a service to our customers we are providing this early version of the manuscript. The manuscript will undergo copyediting, typesetting, and review of the resulting proof before it is published in its final form. Please note that during the production process errors may be discovered which could affect the content, and all legal disclaimers that apply to the journal pertain.

Author Manuscript Author Manuscript Author Manuscript Author Manuscript

mitochondrial fission 48 h after treatment with P-AscH$^-$. P-AscH$^-$ decreased clonogenic survival; this was enhanced by genetic and pharmacological inhibition of both ERK and Drp1. In murine tumor xenografts, the combination of P-AscH$^-$ and pharmacological inhibition of Drp1 increased overall survival. These results suggest that P-AscH$^-$ induces sustained changes in mitochondria, through activation of the ERK/Drp1 signaling pathway, an adaptive response. Inhibition of this pathway enhanced the toxicity P-AscH$^-$ to cancer cells.

Graphical Abstract

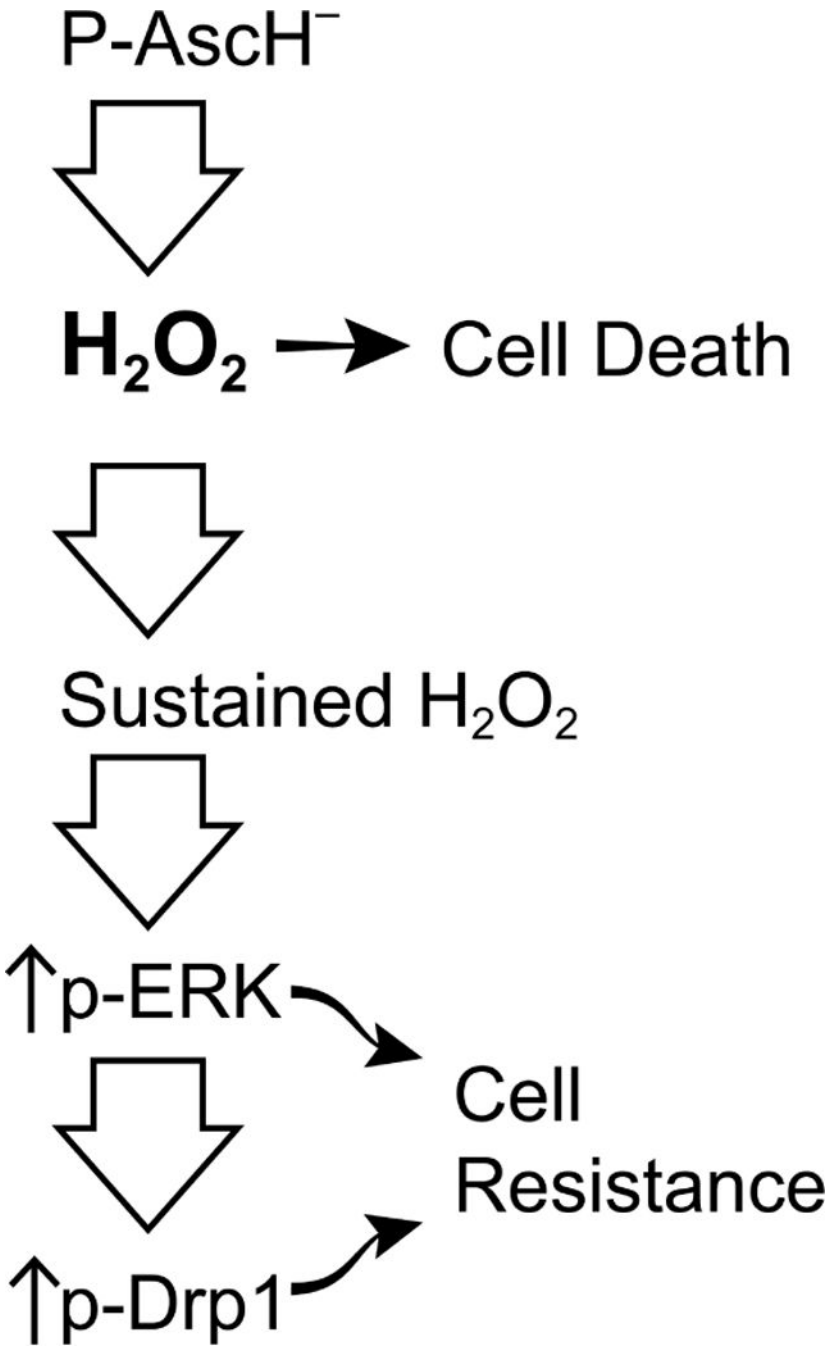

Author Manuscript Author Manuscript Author Manuscript Author Manuscript

Keywords

oxidative stress; pharmacological ascorbate; mitochondrial dynamics; mitochondrial fission

Introduction

Changes in the steady-state levels of reactive oxygen species (ROS) are indicative of the induction of metabolic oxidative stress. For example, previous studies have demonstrated that a sustained increase in radiation-induced steady-state levels of ROS, long-after the initial treatment, results in toxicity while interventions with appropriate antioxidants suppressed the toxicity (1–3). Treatment with pharmacological ascorbate ($P\text{-}AscH^{-}$, high-dose, intravenous vitamin C) results in a transient short-term increase in the flux of hydrogen peroxide (H_2O_2) that is preferentially cytotoxic to cancer cells *vs.* normal cells (4). However, toxicity induced by $P\text{-}AscH^{-}$ is also associated with sustained downstream accumulation of ROS that correlates with toxicity of cancer cells (5). Cellular bioenergetic profiling following exposure to $P\text{-}AscH^{-}$ demonstrated sustained overall changes in mitochondrial function including increased energy demand, basal respiration, ATP-linked oxygen consumption, proton leak, and maximal respiration (5). In addition, these changes were seen in cancer cells, but not in non-tumorigenic cells, suggesting that $P\text{-}AscH^{-}$ as a redox active compound alters signaling pathways involved in cellular propagation.

Emerging evidence supports a crosstalk between redox-sensitive signaling pathways and cellular processes including proliferation and cell death (6–9). For example, many cancers carry KRAS gain-of-function mutations (10) and RAS-RAF-ERK is a major signaling pathway in cancers carrying RAS mutations (11–13). The ERK signaling pathway promotes both proliferation and cell death (6–9). As the terminal master kinase in the MAPK pathway, ERK1/2 phosphorylates hundreds of cytoplasmic and nuclear substrates balancing proliferation and cell death pathways (8,13). Elevated ERK1/2 levels are related to tumorigenesis and have been found in multiple human tumors (14). Patients who are treated with anti-EGF-receptor kinase inhibitors have been found to have ERK2 gene amplification (15), suggesting ERK2 may have a role in treatment resistance and survival.

Recent studies also suggest a regulatory role for ERK-signaling communicating to mitochondrial fission-fusion and mitochondrial functions (16–20). Mitochondrial fission and fusion are known to regulate the shape, size, and number of mitochondria as well as mitochondrial functions (21). Mitochondrial fission-fusion contributes to the cellular redox environment and metabolism with mitochondrial fission associated with a higher glycolytic flux; in contrast, mitochondrial fusion is associated with a higher rate of oxygen consumption (22). Dynamin-related guanosine triphosphatases (GTPases) regulate mitochondrial fission and fusion events (22). Specifically, dynamin-related protein 1 (Drp1) regulates mitochondrial fission and its activity is post-translationally regulated by phosphorylation at S-616 by cyclin B1-CDK1 kinase and at S-637 by protein kinase A (23–25). In cancer cells, ERK phosphorylation of Drp1 (S-616) promotes mitochondrial fission (23,26). Thus, ERK-signaling can influence homeostasis of mitochondrial fission-fusion

Author Manuscript Author Manuscript Author Manuscript Author Manuscript

by phosphorylating Drp1-S616 (positive regulator of fission) or by phosphorylating MFN1-T562 (negative regulator of fusion).

We hypothesized that sustained increases in ROS induced by P-AscH$^-$ are due to redox-sensitive signaling pathways leading to alterations in mitochondrial function. Our data demonstrate that P-AscH$^-$ stimulates increases in phosphorylated ERK and Drp1 that is mediated by H_2O_2, resulting in increased mitochondrial fission. Furthermore, the decrease in clonogenic survival with P-AscH$^-$ was enhanced by genetic and pharmacological inhibition of both ERK and Drp1. In tumor xenografts, the combination of P-AscH$^-$ and pharmacological inhibition of Drp1 increased overall survival.

Methods

Cell Culture--

Human pancreatic ductal adenocarcinoma cell lines MIA PaCa-2 (RRID: CVCL_0428) and PANC-1 (RRID: CVCL_0480) were cultured in DMEM (Gibco, 11965) supplemented with 10% FBS (Gibco, 26140) and 1% penicillin–streptomycin antibiotic (Gibco, 15140). The human patient-derived pancreatic ductal adenocarcinoma cell line 339 was cultured in DMEM/F-12 media (Gibco, 11320) supplemented with 10% FBS, insulin (Gibco, 12585), EGF (Gibco, PHG0311), hydrocortisone (Sigma, H0888), bovine pituitary extract (Gibco, 13028), and 1% penicillin–streptomycin antibiotic. Nontumorigenic HPV16-E6E7-immortalized cell line derived from normal pancreatic ductal epithelium (H6c7) (RRID: CVCL_0P38) with near normal genotype and phenotype of pancreatic duct epithelial cells were used for comparison. H6c7 cells were cultured in Serum Free Keratinocyte media (Gibco, 10724) supplemented with EGF (1 ng/mL), bovine pituitary extract (50 mg/mL), and 1% penicillin–streptomycin antibiotic. Human cell lines (MIA PaCa-2, PANC-1, and H6c7) were purchased directly from the ATCC and were passaged for fewer than 6 months after receipt. No additional authentication was performed. The patient-derived cell line (PDX339) was obtained from the Medical College of Wisconsin surgical oncology tissue bank (27). In addition, MIA PaCa-2 cells were transfected with plasmids containing mUNG1 (pMA3790, RRID: Addgen_70110) or HSV-1 UL12.5M185 (pMA4008, RRID: Addgene_70109) gene to generate cells without functional mitochondria (ρ^0 cells) (28). Mitochondrial expression of DNA repair enzymes mutant Y147A human uracil-N-glycosylase (mUNG1) or Herpes Simplex Virus 1 (HSV-1) protein UL12.5M185 leads to mtDNA depletion and the formation of ρ^0 cells. ρ^0 cells were grown in DMEM containing 10% FBS, 50 μg/mL uridine and 1 mM sodium pyruvate. Pyruvate was removed prior to treatment with P-AscH$^-$ as pyruvate can scavenge H_2O_2 (29). Frozen cell lines were routinely tested for mycoplasma. Regardless of varying cell type and media components, all cells were treated in fresh 10% DMEM media with ascorbate for 1 h at 37 °C. After the 1 h treatment, media were replaced, *i.e.*, P-AscH$^-$ was removed, and cells were allowed to incubate for 48 h. P-AscH$^-$ came from a stock solution of 1.00 M (pH 7) made under argon and stored with a tight-fitting stopper at 4 °C. Ascorbate concentration was verified at 265 nm, $\varepsilon 265 = 14{,}500\ M^{-1}\ cm^{-1}$(30). To enhance rigor and reproducibility, final concentrations of the exposure to cells were calculated in units of moles-per-cell to account for variation in media, cell density, and cellular metabolism (31).

Author Manuscript Author Manuscript Author Manuscript Author Manuscript

Clonogenic Survival--

Clonogenic survival assays were performed as previously described (4). Approximately 1–3 × 10^5 cells were seeded 1 d prior to assay. Cells were treated with P-AscH$^-$ (10–30 pmol/cell, 1–2 mM, LD_{50} for each individual cell line) for 1 h in DMEM/10% FBS followed by SCH772984 (Selleckchem, S7101) or Mdivi-1 (Sigma, M0199) for 24 h. Cells have different susceptibility to P-AscH$^-$ (31). Thus, the LD_{50} for clonogenic survival for each cell line was used as a guide to determine appropriate doses of P-AscH$^-$ to use in the various experiments. Cells were trypsinized with TrypLE Express (Gibco, 12604) to form a single-cell suspension and counted using a Countess II automated cell counter (Thermo Fisher) to determine the number of cells plated into each well. Cells were allowed to form colonies for 7 to 14 d before being fixed with 70% ethanol and stained with Coomassie Blue. Colonies containing ≥ 50 cells were scored. Surviving fraction was defined as number of colonies counted/number of cells seeded. Each experimental condition was normalized to their own control to determine a normalized surviving fraction. Experiments were repeated in triplicate.

Western blotting--

Protein samples were isolated and prepared in phosphosafe buffer (EDM Millipore, 71296) containing protease inhibitor cocktail (Sigma Aldrich). Protein content was measured using a DC Protein assay. Total protein (10–40 mg) was loaded on a 4%−20% SDS-PAGE gradient gel. Protein was transferred to Immun-Blot PVDF membrane (Bio-Rad). Membranes were blocked in 5% BSA in PBST. Primary antibodies included: P-ERK (1:1000; #4370, Cell Signaling), ERK (1:1000; #4695, Cell Signaling), Drp1 (1:1000; #5391S, Cell Signaling), P-Drp1 (1:1000; #4494S, Cell Signaling), tubulin (1:2,000; #E7; University of Iowa Developmental Studies Hybridoma Bank, RRID: AB_528499), and GAPDH (1:5,000; #14C10, Cell Signaling). Appropriate horseradish peroxidase–linked secondary antibodies were used at a concentration of 1:20,000. Blots were visualized with SuperSignal West Pico substrate (Thermo Scientific, 34579) on x-ray film. Quantification of the *in vivo* sample westerns was performed by comparing fraction of p-ERK/ERK. Normalized average integrated densities were determined with ImageJ software (RRID: SCR_003070).

Confocal Microscopy for mitochondrial compartments and volume--

Cells were treated with P-AscH$^-$ for 1 h, then incubated for 48 h. Cells were then labeled with 100 nM MitoTracker© Green FM for 20 min in DMEM phenol-red free medium. Confocal fluorescence images were taken with Zeiss LSM710. Imaris Image Analysis Software (Bitplane) was used to create images of the mitochondrial network and to calculate mitochondrial volume and number of compartments.

Confocal Microscopy for colocalization of in vivo samples--

Tumor samples were fixed with 4% paraformaldehyde in 0.1 M PBS at 4 ° C overnight. Samples were embedded in OCT and 8 μm sections were cut in a Thermo HM525 Cryostat (Thermo Scientific). OCT sections were warmed up to room temperature and washed with PBS before blocking with 5% normal goat serum (NGS) for 30 min. Sections were incubated with mitochondrial cytochrome c oxidase 1 mouse antibody (1:50, Abcam, RRID:

Author Manuscript Author Manuscript Author Manuscript Author Manuscript

AB_2084810) and p-Drp1 (Ser616) rabbit antibody (1:50, #4494S Cell Signaling) in 1% NGS overnight at 4 ° C. An Alexa Flour 488 conjugated goat anti-mouse (1:200, RRID: AB_10892893) or goat anti-rabbit (Alexa Flour 568 conjugated) was used as secondary antibody. DAPI was used to stain the cell nuclei. Tumor tissue sections were examined with a Zeiss LSM710 confocal microscope (Central Microscopy Research Facility, University of Iowa).

Electron Microscopy--

MIA PaCa-2 cells grown on 18 mm glass cover slips in a 12-well plate treated with P-AscH$^-$ 1 mM (15 pmol/cell) for 1 h. After treatment, cells were cultured in fresh growth media for 48 h, then were fixed in 2.5% glutaraldehyde in 0.1 M cacodylate buffer, pH 7.4 overnight at 4 °C. After several 0.1 M cacodylate buffer rinses, cells were stained in 0.1% tannic acid followed by post-fixation in 1% OsO_4 in 0.1 M cacodylate buffer plus 0.8% potassium ferricyanide, and then post fixed with 1% OsO_4 for 1 h. Following serial alcohol dehydration (50%, 75%, 95%, and 100%), the samples were embedded in Epon 12 (Ted Pella). Ultramicrotomy was performed, and ultrathin sections (70 nm) were post stained with uranyl acetate and lead citrate. Samples were visualized with a JEOL 1230 transmission electron microscope (TEM) at the Central Microscopy Research Facility of The University of Iowa.

siRNA Transfection--

Transfection of siRNA was carried out using a Lipofectamine 2000 Reagent (Life Technologies) according to manufacturer's direction. Briefly, cells (1.5×10^5 /well) were seeded in 6-well tissue culture plates, Lipofectamine and siRNA (100 nmol) were diluted in Opti-MEM reduced serum medium before mixing; the transfection complex was incubated at room temperature for 5 min before adding to the cells. Clonogenic assays and western blotting were performed 48 h after transfection. Drp1 siRNA was purchased from Santa Cruz Biotechnology, siERK (p44/42) and control siRNA were from Cell Signaling.

In vivo experiments--

The animal protocols were reviewed and approved by the Animal Care and Use Committee of The University of Iowa. Thirty-day-old female athymic nude mice (*Foxn1*^{nu}) were obtained from Envigo (RRID: RGD_5508395). Animals were acclimated in the unit for 1 week before any manipulations were performed. For experiments growing xenografts with MIA PaCa-2 cells (2×10^6), tumors were delivered subcutaneously into each flank region of nude mice with a 1-mL tuberculin syringe equipped with a 25-gauge needle. Tumor size was measured every two to three days by means of a vernier caliper, and tumor volume was estimated according to the following formula: tumor volume = Π/6 x L x W^2, where L is the greatest dimension of the tumor, and W is the dimension of the tumor in the perpendicular direction Tumors were allowed to grow to approximately 5 mm in diameter before experimental treatment began. For tumor isolation experiments for Drp1 colocalization, mice were treated P-AscH$^-$ (4 g/kg, i.p., b.i.d.) or an equivalent volume of saline (1 mol/L) for 5 d. Mice were euthanized by CO_2 asphyxiation, and tumors were harvested and processed for experimental analyses. For survival experiments, mice were treated daily for 21 d with P-AscH$^-$ (4 g/kg, i.p.) while mitochondrial division inhibitor-1

Author Manuscript Author Manuscript Author Manuscript Author Manuscript

(Mdivi-1) was administered i.p. 50 mg/kg. Mice body weights were measured twice per week during the treatment period.

Statistical methods--

Data are presented as the mean ± SEM. For statistical analyses of two groups, unpaired two tailed Student t tests were utilized. To study statistical differences between multiple comparisons, significance was determined using one-way ANOVA analysis with Tukey multiple comparisons test. For survival curve analysis, Log-rank (Mantel-Cox) test was used to compare median survival. All analyses were performed in GraphPad Prism (GraphPad Software, Inc.; RRID: SCR_002798).

Results

P-AscH$^-$-induced ERK and Drp1 activation is mediated by H_2O_2--

Phosphorylated ERK1/2 (p-ERK) is the active form of ERK known to activate Drp1, a GTPase protein which alters mitochondrial morphology by inducing fission. Western blot analysis showed that treatment for 1 h with P-AscH$^-$ (1–2 mM) induced an increase in p-ERK 48 h after treatment in the 339 (Figure 1A) and the MIA PaCa-2 (Figure 1B) PDAC cell lines. This increase in p-ERK was not observed in the nontumorigenic H6c7 pancreatic ductal epithelial cell line (Figure 1C). A time course experiment using the MIA PaCa-2 cell line confirmed that the increases in p-ERK (Figure 1D) and p-Drp1 (Figure 1E) do not occur until 48 h after treatment with P-AscH$^-$. Previous studies have shown that catalase reverses the cytotoxic effects of P-AscH$^-$, consistent with a H_2O_2-mediated mechanism of selective toxicity to PDAC cells (4). Treatment of MIA PaCa-2 cells with catalase (100 μg/mL) prior to treatment with P-AscH$^-$ reversed the increase in p-Drp1 and p-ERK (Figure 1F). These data suggest that the P-AscH$^-$-induced increases in p-ERK and p-Drp1 are mediated by H_2O_2. To investigate if the P-AscH$^-$-induced increases in p-ERK occur *in vivo*, established tumor PANC-1 xenografts were treated with P-AscH$^-$ (4g/kg i.p., b.i.d.) or saline (1.0 M IP daily) for 5 d. Tumor samples harvested from P-AscH$^-$-treated mice demonstrated increases in p-ERK protein (Figure 1G) and increases in the p-ERK/ERK ratio compared to tumor samples from mice treated with saline (Figure 1H).

P-AscH$^-$ induces mitochondrial fission and Drp1 activation--

Activated ERK is known to activate Drp1 *via* phosphorylation of Ser 616. Once activated, Drp1 is recruited to the mitochondria and found in the mitochondrial outer membrane (32). ERK phosphorylation of Drp1 promotes mitochondrial fission (23). Since P-AscH$^-$ increased p-Drp1 levels 48 h after treatment in PDAC cells, we sought to test whether P-AscH$^-$ would induce mitochondrial fission 48 h after treatment. Mito Tracker staining was used to measure the number of compartments and total volume of mitochondria 48 h after PDAC cells were treated with P-AscH$^-$ (10 pmole/cell, 1 mM) P-AscH$^-$ decreased total volume and increased the number of compartments consistent with mitochondrial fission (Figure 2A, B). These studies were repeated in the PDX339 PDAC cell line demonstrating a 1.4-fold increase in the number of compartments with P-AscH$^-$ (data not shown). To support that these changes in mitochondrial morphology were consistent with fission, electron microscopy (Figure 2C) demonstrated decreased length of mitochondria following P-AscH$^-$

Author Manuscript Author Manuscript Author Manuscript Author Manuscript

compared to controls. Quantification demonstrated significant decreases in mitochondrial length in P-AscH$^-$ treated cells (Figure 2D), also consistent with mitochondrial fission. Finally, to determine if these increases in mitochondrial fragmentation correlated with the activation of Drp1, we measured colocalization of p-Drp1 to the mitochondria in tumor xenografts from mice treated with P-AscH$^-$ or saline. Tumor xenografts were stained for p-Drp1 and mitochondrial cytochrome c oxidase (Figure 2E). In tumor xenografts treated with P-AscH$^-$, p-Drp1 colocalization with cytochrome c oxidase was increased compared to saline treated animals (Figure 2F), signifying increased Drp1 colocalization to the mitochondria. These data suggest that P-AscH$^-$-induced increases in mitochondrial fission that correlates with activation of Drp1.

Genetic inhibition of ERK and Drp1 sensitizes cancer cells to P-AscH$^-$--

To determine the role of P-AscH$^-$ in the activation of ERK and Drp1, we generated cell lines using siRNA to inhibit both ERK and Drp1. A significant decrease in p-ERK protein in MIA PaCa-2 cells generated using the siRNA transfection was observed (Figure 3A). Because there is a regulatory role for ERK-signaling communicating to mitochondrial fission-fusion process and Drp1 activation (16,17), the siERK knockout also demonstrated decreases in the activation of Drp1 (Figure 3A).

Parental and siRNA cell lines were then treated with P-AscH$^-$ (7 pmole/cell) for 1 h to determine clonogenic survival. Genetic inhibition of ERK significantly increased the effects on P-AscH$^-$-induced reduction in clonogenic survival (Figure 3B) compared to siNEG and controls. We then generated cells with inhibition of Drp1 using siRNA technology; western blotting verified decreased levels of activated Drp1 (Figure 3C). Clonogenic survival demonstrated that cells with genetic inhibition of Drp1 were significantly more sensitive to P-AscH$^-$ compared to their siNEG and controls (Figure 3D). These data suggest that the activation of ERK/Drp1 may be a survival response when exposed to P-AscH$^-$, and inhibition of this pathway may render cancer cells more sensitive to P-AscH$^-$.

No change in p-ERK or p-Drp1 following P-AscH$^-$ in ρ^0 cells lacking oxidative phosphorylation–ρ^0 cells derived from the MIA PaCa-2 cell line were utilized to evaluate the effects that P-AscH$^-$ might have on p-ERK and p-Drp1 expression in the absence of mitochondria (28). Two different ρ^0 clones, clone 3 and clone 4, were treated with 10 pmole/cell (1 mM) P-AscH$^-$ for 1 h and then allowed to proliferate for 48 h prior to protein isolation. Unlike MIA PaCa-2 and PANC-1 cells that demonstrate dose- and time-dependent increases in p-ERK and p-Drp1 following treatment with P-AscH$^-$, the ρ^0 cells did not demonstrate any change in p-ERK or p-Drp1 protein expression compared to control (Figure 4). These results suggest that P-AscH$^-$ acts at the mitochondrial level to induce cell stress and promotes mitochondrial fission in cancer cells. Previous studies have demonstrated that these ρ^0 cell lines are resistant to P-AscH$^-$, further suggesting that the p-ERK/p-DRP1 pathway is dependent upon functional mitochondria and thus may be partially responsible for cancer cell resistance to P-AscH$^-$ treatment (28).

Author Manuscript Author Manuscript Author Manuscript Author Manuscript

Pharmacological Inhibition of ERK or Drp1 sensitizes cancer cells to P-AscH$^-$--

Morris *et al.* have described a novel selective ERK1/2 inhibitor, SCH772984, that demonstrated tumor regression in xenograft models of BRAF, NRAS, and KRAS mutant tumors (33). This inhibitor also effectively inhibited MAPK-signaling in tumor cells that had developed resistance to inhibitors of BRAF or MEK (33). Pancreatic cancer and H6c7 cells were treated with P-AscH$^-$ (1 mM for 1 h), SCH772984 (1 μM for 24 h), or a combination of P-AscH$^-$ and SCH772984. SCH772984 prevented the P-AscH$^-$-induced increased phosphorylation of ERK (Figure 5A), but also prevented the increased phosphorylation of downstream Drp1 (Figure 5B). Cancer cells treated with P-AscH$^-$ alone or SCH772984 alone had decreased clonogenic survival compared to controls in both cancer cell lines MIA PaCa-2 (Figure 5C) and PDX339 (Figure 5D); clonogenic survival was further reduced when the two compounds were used in a combined treatment. The non-tumorigenic pancreatic ductal epithelial cell line H6c7 cells did not demonstrate a decrease in clonogenic survival with treatment by either P-AscH$^-$ alone, SCH772984 alone, or with the P-AscH$^-$ and SCH772984 combination treatment (Figure 5E). These data combined with the results of the genetic manipulation by siERK indicate that inhibition of the ERK pathway sensitizes cancer cells to P-AscH$^-$.

The mitochondrial division inhibitor-1 (Mdivi-1) has been shown to inhibit mitochondrial fission, increase mitochondrial fusion, and thereby increase mitochondrial length (34). Mdivi (25 and 50 μM) reversed the P-AscH$^-$-induced phosphorylation of Drp1 in MIA PaCa-2 cells (Figure 6A). PDAC and H6c7 cells were then treated with P-AscH$^-$ (1 mM for 1 h), Mdivi-1 (50 μM for 24 h), or P-AscH$^-$ + Mdivi-1 to determine clonogenic survival. Like the findings with the genetic inhibition of Drp1, combining P-AscH$^-$ with Mdivi-1 resulted in significant decreases in clonogenic survival compared to either treatment alone (Figure 6B, C). As seen in the previous experiments, H6c7 cells were not sensitive to any of the treatments (Figure 6D).

Mdivi-1 plus P-AscH$^-$ improves survival in PDAC xenografts--

Mdivi-1 has previously been shown to inhibit the growth of pancreatic cancer *in vivo* (35). To test whether the combination of P-AscH$^-$ and Mdivi-1 would increase survival, MIA PaCA-2 xenografts were generated. When tumors were 5 mm in diameter, mice were randomized to receive daily treatment of either saline, P-AscH$^-$ (4 g/kg i.p.), Mdivi-1 (50 mg/kg i.p.), or P-AscH$^-$ + Mdivi-1 for 21 d. Compared to controls, mice in the combination treatment group had the longest median survival (54 *vs.* 33 days, $*p < 0.05$) (Figure 7A). The treatments were well tolerated with no signs of toxicities and no significant differences in body weight between groups (Figure 7B). Also, Mdivi-1 + P-AscH$^-$ decreased phosphorylated Drp1 in tumor xenografts as measured by immunofluorescence (Figure 7C) and quantified by immunofluorescence (Figure 7D) ($*p < 0.05$ *vs.* control, means ± SEM). These survival data are consistent with our *in vitro* models of genetic and pharmacological Drp1 inhibition, suggesting that pharmacological inhibition of Drp1 *in vivo* sensitizes cancer cells to P-AscH$^-$.

Author Manuscript Author Manuscript Author Manuscript Author Manuscript

Discussion

Many cancers rely on energy produced by oxidative phosphorylation from the mitochondria to grow and metastasize (36). Mitochondria within a cell can collectively alter their structures to optimize their metabolic functions in response to cellular insults (37). One such process is mitochondrial fusion, which is critical for organelle function (38). In response to oxidative stress, mitochondria can fragment into smaller organelles through mitochondrial fission (39). These mitochondrial dynamics of fission and fusion in response to oxidative stress is regulated by a few key proteins including the GTPase Drp1 which regulates mitochondrial fission, and its dysfunction may promote unregulated mitochondrial fusion (40).

One of the strengths of our current study is the use of pancreatic cancer cells, which exhibit highly fragmented mitochondria (41); this fragmentation suggests basal mitochondrial dynamics that favor mitochondrial fission. Previous studies by Serasinghi and colleagues (26) demonstrated that shifting the balance of mitochondrial dynamics toward mitochondrial fusion in pancreatic cancer cells normalizes their function and reduces oncogenicity. This approach may be promising since mitochondrial fusion is more frequently observed in normal cells (42). Previous studies by Yu *et al.* have also found that the genetic or pharmacologic activation of mitochondrial fusion reduces growth and improves survival in mouse models of pancreatic cancer (35). Combined with our current study utilizing P-AscH$^-$, these results demonstrate the critical role of mitochondria and how they could be potentially exploited therapeutically. Our current study is also consistent with recent studies in our laboratory demonstrating extensive changes in mitochondrial metabolism after treatment with P-AscH$^-$, suggesting that cancer cells that largely use oxidative phosphorylation to generate ATP may be more sensitive to P-AscH$^-$ compared with cells that are glycolysis-dependent (28).

Although still in phase II trials, P-AscH$^-$, which we have shown to be safe and possibly efficacious . Pharmacological doses of ascorbate (2 – 20 mM for 1 h; 5–100 g administered intravenously) is cytotoxic to cancer cells, but not to normal cells, *via* generation of H_2O_2 (4). When given intravenously, plasma levels of ascorbate can reach up to 20–30 mM. These levels are not attainable with oral delivery, which reaches maximum levels of around 0.2 mM.

The prevalence of *KRAS* driven tumorigenesis in cancer has also spurred many investigations into the potential targets within the RAS-RAF-MEK-ERK pathway. Our current study demonstrates that P-AscH$^-$, *via* H_2O_2 generation, activates ERK which activates Drp1. This leads to increased mitochondrial fission, which correlates with previous studies demonstrating sustained increases in mitochondrial oxygen consumption 48 h after treatment with P-AscH$^-$ (5). Inhibiting the ERK/Drp1 pathway either genetically or pharmacologically sensitized cancer cells to P-AscH$^-$, suggesting that ERK/Drp1 activation may be a resistance mechanism.

Many pancreatic, lung and colon cancers have a mutational activation of *KRAS* (10). The downstream signaling cascade activated by *KRAS* includes RAF-MEK-ERK, the

Author Manuscript Author Manuscript Author Manuscript Author Manuscript

activation of which promotes cell growth, survival, and proliferation. Targeting *KRAS* and its downstream kinases have therefore been the subject of many studies aiming to improve outcomes of cancer treatment. Unfortunately, these therapies so far have been unsuccessful in improving survival in clinical trials. For example, an oral farnesyl transferase inhibitor, which inhibits a key step in RAS activation, did not improve survival in a phase II trial (43). RAF and MEK kinases, which are downstream of RAS, were also thought to be promising targets to disrupt the MAPK pathway in pancreatic cancer as they both have limited substrate specificities. However, RAF and MEK inhibitors have also failed to demonstrate effectiveness in improving pancreatic cancer survival (44,45). These inhibitors have been found to induce resistance through mechanisms that enable recovery of the MAPK pathway. Specifically, RAF inhibitors were ineffective in RAS-mutant cancers due to paradoxical RAS-dependent RAF dimerization and activation, leading to enhanced ERK activation (46). Similarly, MEK inhibitors induce resistance through compensatory mechanisms that activate ERK. Therapies that combine inhibitors of BRAF/MEK have also failed to escape this resistance pattern through ERK activation (47,48). In *KRAS* mutant pancreatic cancers, inhibition of ERK is known to express anti-tumor activity *in vitro* (49,50). Our results not only support this, but also show that combining P-AscH$^-$ with inhibition of ERK is even more cytotoxic to cancer cells.

Our findings also encourage efforts to investigate perturbations in mitochondrial dynamics as a targetable feature. Anderson *et al.* demonstrated alterations in proteins that regulate mitochondrial dynamics sensitizes cancer cells to a variety of drugs (41). Our present study demonstrates that inhibition of ERK and Drp1, which disrupts mitochondrial fission, sensitizes cancer cells to P-AscH$^-$. Our current study used Mdivi-1 as a Drp1 inhibitor; our findings are consistent with studies demonstrating Mdivi-1 inhibition of tumor growth in genetic mouse models of pancreatic cancer (35). Another avenue for exploiting mitochondrial dynamics in PDAC has been through inducing mitochondrial fusion instead of inhibiting fission. In the same study, Yu and colleagues demonstrated increased mitochondrial fusion led to decreased growth and increased survival in the genetic mouse model of pancreatic cancer (35).

Previous studies have demonstrated that P-AscH$^-$-induced toxicity is due to immediate generation of H_2O_2 from ascorbate oxidation. However, P-AscH$^-$-induced toxicity may also be enhanced by late metabolic shifts in tumor cells resulting in a feed-forward mechanism for generation of H_2O_2 and induction of metabolic stress through enhanced Dual Oxidase expression and increased rate of oxygen consumption (5). Our current study expands these observations by demonstrating that P-AscH$^-$, *via* sustained H_2O_2 generation, activates the ERK pathway resulting in changes in mitochondrial dynamics (Figure 8). Inhibiting this pathway renders cancer cells more sensitive to P-AscH$^-$, suggesting that ERK activation may be a resistance mechanism in cells treated with P-AscH$^-$ and that the addition of P-AscH$^-$ to novel ERK/Drp1 inhibitors may be a promising additive or synergistic therapy.

ACKNOWLEDGEMENTS

Supported by NIH grants P01CA217797, P30CA086862, and CA148062. The authors would like to acknowledge use of the University of Iowa Central Microscopy Research Facility and the ESR Facility, the Holden Comprehensive Cancer Center and the Carver College of Medicine.

Author Manuscript Author Manuscript Author Manuscript Author Manuscript

Supported by NIH grants P01 CA217797, CA148062, and CA184051

References

1. Fisher CJ, Goswami PC. Mitochondria-targeted antioxidant enzyme activity regulates radioresistance in human pancreatic cancer cells. Cancer biology & therapy. Aug 2008;7(8):1271–1279. [PubMed: 18497575]
2. Gao Z, Sarsour EH, Kalen AL, Li L, Kumar MG, Goswami PC. Late ROS accumulation and radiosensitivity in SOD1-overexpressing human glioma cells. Free radical biology & medicine. Dec 1 2008;45(11):1501–1509. [PubMed: 18790046]
3. Eckers JC, Kalen AL, Xiao W, Sarsour EH, Goswami PC. Selenoprotein P inhibits radiation-induced late reactive oxygen species accumulation and normal cell injury. International journal of radiation oncology, biology, physics. Nov 1 2013;87(3):619–625. [PubMed: 24074935]
4. Du J, Martin SM, Levine M, Wagner BA, Buettner GR, Wang SH, et al. Mechanisms of ascorbate-induced cytotoxicity in pancreatic cancer. Clinical cancer research : an official journal of the American Association for Cancer Research. Jan 15 2010;16(2):509–520. [PubMed: 20068072]
5. Gibson AR, O'Leary BR, Du J, Sarsour EH, Kalen AL, Wagner BA, et al. Dual Oxidase-Induced Sustained Generation of Hydrogen Peroxide Contributes to Pharmacological Ascorbate-Induced Cytotoxicity. Cancer research. Feb 10 2020.
6. Che TF, Lin CW, Wu YY, Chen YJ, Han CL, Chang YL, et al. Mitochondrial translocation of EGFR regulates mitochondria dynamics and promotes metastasis in NSCLC. Oncotarget. Nov 10 2015;6(35):37349–37366. [PubMed: 26497368]
7. Choudhary S, Wang KK, Wang HC. Oncogenic H-Ras, FK228, and exogenous H2O2 cooperatively activated the ERK pathway in selective induction of human urinary bladder cancer J82 cell death. Mol Carcinog. Mar 2011;50(3):215–219.
8. Cook SJ, Stuart K, Gilley R, Sale MJ. Control of cell death and mitochondrial fission by ERK1/2 MAP kinase signalling. Febs j. Dec 2017;284(24):4177–4195. [PubMed: 28548464]
9. Ying H, Kimmelman AC, Lyssiotis CA, Hua S, Chu GC, Fletcher-Sananikone E, et al. Oncogenic Kras maintains pancreatic tumors through regulation of anabolic glucose metabolism. Cell. Apr 27 2012;149(3):656–670. [PubMed: 22541435]
10. Bryant KL, Mancias JD, Kimmelman AC, Der CJ. KRAS: feeding pancreatic cancer proliferation. Trends Biochem Sci. Feb 2014;39(2):91–100. [PubMed: 24388967]
11. Eser S, Schnieke A, Schneider G, Saur D. Oncogenic KRAS signalling in pancreatic cancer. Br J Cancer. Aug 26 2014;111(5):817–822. [PubMed: 24755884]
12. Hu Y, Lu W, Chen G, Wang P, Chen Z, Zhou Y, et al. K-ras(G12V) transformation leads to mitochondrial dysfunction and a metabolic switch from oxidative phosphorylation to glycolysis. Cell Res. Feb 2012;22(2):399–412.
13. Weinberg F, Hamanaka R, Wheaton WW, Weinberg S, Joseph J, Lopez M, et al. Mitochondrial metabolism and ROS generation are essential for Kras-mediated tumorigenicity. Proceedings of the National Academy of Sciences of the United States of America. May 11 2010;107(19):8788–8793. [PubMed: 20421486]
14. Guo YJ, Pan WW, Liu SB, Shen ZF, Xu Y, Hu LL. ERK/MAPK signalling pathway and tumorigenesis. Exp Ther Med. Mar 2020;19(3):1997–2007. [PubMed: 32104259]
15. Ercan D, Xu C, Yanagita M, Monast CS, Pratilas CA, Montero J, et al. Reactivation of ERK signaling causes resistance to EGFR kinase inhibitors. Cancer Discov. Oct 2012;2(10):934–947. [PubMed: 22961667]
16. Chan DC. Fusion and fission: interlinked processes critical for mitochondrial health. Annu Rev Genet. 2012;46:265–287. [PubMed: 22934639]
17. Chen H, Chomyn A, Chan DC. Disruption of fusion results in mitochondrial heterogeneity and dysfunction. The Journal of biological chemistry. Jul 15 2005;280(28):26185–26192. [PubMed: 15899901]
18. Chen H, Vermulst M, Wang YE, Chomyn A, Prolla TA, McCaffery JM, et al. Mitochondrial fusion is required for mtDNA stability in skeletal muscle and tolerance of mtDNA mutations. Cell. Apr 16 2010;141(2):280–289. [PubMed: 20403324]

Author Manuscript Author Manuscript Author Manuscript Author Manuscript

19. Dal Yontem F, Kim SH, Ding Z, Grimm E, Ekmekcioglu S, Akcakaya H. Mitochondrial dynamic alterations regulate melanoma cell progression. J Cell Biochem. Sep 6 2018.
20. Nagdas S, Kashatus JA, Nascimento A, Hussain SS, Trainor RE, Pollock SR, et al. Drp1 Promotes KRas-Driven Metabolic Changes to Drive Pancreatic Tumor Growth. Cell Rep. Aug 13 2019;28(7):1845–1859.e1845. [PubMed: 31412251]
21. Chen H, Chan DC. Mitochondrial dynamics--fusion, fission, movement, and mitophagy-in neurodegenerative diseases. Hum Mol Genet. Oct 15 2009;18(R2):R169–176. [PubMed: 19808793]
22. Xiao W, Sarsour EH, Wagner BA, Doskey CM, Buettner GR, Domann FE, et al. Succinate dehydrogenase activity regulates PCB3-quinone-induced metabolic oxidative stress and toxicity in HaCaT human keratinocytes. Arch Toxicol. Feb 2016;90(2):319–332. [PubMed: 25417049]
23. Kashatus DF, Lim KH, Brady DC, Pershing NL, Cox AD, Counter CM. RALA and RALBP1 regulate mitochondrial fission at mitosis. Nat Cell Biol. Aug 7 2011;13(9):1108–1115. [PubMed: 21822277]
24. Liesa M, Palacín M, Zorzano A. Mitochondrial dynamics in mammalian health and disease. Physiol Rev. Jul 2009;89(3):799–845. [PubMed: 19584314]
25. Taguchi N, Ishihara N, Jofuku A, Oka T, Mihara K. Mitotic phosphorylation of dynamin-related GTPase Drp1 participates in mitochondrial fission. The Journal of biological chemistry. Apr 13 2007;282(15):11521–11529. [PubMed: 17301055]
26. Serasinghe MN, Wieder SY, Renault TT, Elkholi R, Asciolla JJ, Yao JL, et al. Mitochondrial division is requisite to RAS-induced transformation and targeted by oncogenic MAPK pathway inhibitors. Mol Cell. Feb 5 2015;57(3):521–536. [PubMed: 25658204]
27. Roy I, Zimmerman NP, Mackinnon AC, Tsai S, Evans DB, Dwinell MB. CXCL12 chemokine expression suppresses human pancreatic cancer growth and metastasis. PloS one. 2014;9(3):e90400. [PubMed: 24594697]
28. Du J, Pope AN, O'Leary BR, Wagner BA, Goswami PC, Buettner GR, et al. The role of mitochondria in pharmacological ascorbate-induced toxicity. Scientific reports. Dec 29 2022;12(1):22521. [PubMed: 36581766]
29. Olney KE, Du J, van 't Erve TJ, Witmer JR, Sibenaller ZA, Wagner BA, et al. Inhibitors of hydroperoxide metabolism enhance ascorbate-induced cytotoxicity. Free Radical Research. 2013/03/01 2013;47(3):154–163. [PubMed: 23205739]
30. Buettner GR. In the absence of catalytic metals ascorbate does not autoxidize at pH 7: ascorbate as a test for catalytic metals. Journal of biochemical and biophysical methods. May 1988;16(1):27–40. [PubMed: 3135299]
31. Doskey CM, Buranasudja V, Wagner BA, Wilkes JG, Du J, Cullen JJ, et al. Tumor cells have decreased ability to metabolize H2O2: Implications for pharmacological ascorbate in cancer therapy. Redox biology. Dec 2016;10:274–284. [PubMed: 27833040]
32. Frank S, Gaume B, Bergmann-Leitner ES, Leitner WW, Robert EG, Catez F, et al. The role of dynamin-related protein 1, a mediator of mitochondrial fission, in apoptosis. Dev Cell. Oct 2001;1(4):515–525. [PubMed: 11703942]
33. Morris EJ, Jha S, Restaino CR, Dayananth P, Zhu H, Cooper A, et al. Discovery of a novel ERK inhibitor with activity in models of acquired resistance to BRAF and MEK inhibitors. Cancer Discov. Jul 2013;3(7):742–750. [PubMed: 23614898]
34. Cassidy-Stone A, Chipuk JE, Ingerman E, Song C, Yoo C, Kuwana T, et al. Chemical inhibition of the mitochondrial division dynamin reveals its role in Bax/Bak-dependent mitochondrial outer membrane permeabilization. Dev Cell. Feb 2008;14(2):193–204. [PubMed: 18267088]
35. Yu M, Nguyen ND, Huang Y, Lin D, Fujimoto TN, Molkentine JM, et al. Mitochondrial fusion exploits a therapeutic vulnerability of pancreatic cancer. JCI Insight. Jul 23 2019;5(16).
36. Viale A, Pettazzoni P, Lyssiotis CA, Ying H, Sánchez N, Marchesini M, et al. Oncogene ablation-resistant pancreatic cancer cells depend on mitochondrial function. Nature. Oct 30 2014;514(7524):628–632. [PubMed: 25119024]
37. Chen H, Chan DC. Mitochondrial Dynamics in Regulating the Unique Phenotypes of Cancer and Stem Cells. Cell Metab. Jul 5 2017;26(1):39–48. [PubMed: 28648983]

Author Manuscript Author Manuscript Author Manuscript Author Manuscript

38. Youle RJ, van der Bliek AM. Mitochondrial Fission, Fusion, and Stress. Science (New York, N.Y.). 2012;337(6098):1062–1065. [PubMed: 22936770]
39. Boland ML, Chourasia AH, Macleod KF. Mitochondrial dysfunction in cancer. Front Oncol. Dec 2 2013;3:292. [PubMed: 24350057]
40. Zhao J, Zhang J, Yu M, Xie Y, Huang Y, Wolff DW, et al. Mitochondrial dynamics regulates migration and invasion of breast cancer cells. Oncogene. Oct 2013;32(40):4814–4824. [PubMed: 23128392]
41. Anderson GR, Wardell SE, Cakir M, Yip C, Ahn YR, Ali M, et al. Dysregulation of mitochondrial dynamics proteins are a targetable feature of human tumors. Nat Commun. Apr 26 2018;9(1):1677. [PubMed: 29700304]
42. Luchsinger LL, de Almeida MJ, Corrigan DJ, Mumau M, Snoeck HW. Mitofusin 2 maintains haematopoietic stem cells with extensive lymphoid potential. Nature. Jan 28 2016;529(7587):528–531. [PubMed: 26789249]
43. Macdonald JS, McCoy S, Whitehead RP, Iqbal S, Wade JL 3rd, Giguere JK, et al. A phase II study of farnesyl transferase inhibitor R115777 in pancreatic cancer: a Southwest oncology group (SWOG 9924) study. Invest New Drugs. Oct 2005;23(5):485–487. [PubMed: 16133800]
44. Infante JR, Somer BG, Park JO, Li CP, Scheulen ME, Kasubhai SM, et al. A randomised, double-blind, placebo-controlled trial of trametinib, an oral MEK inhibitor, in combination with gemcitabine for patients with untreated metastatic adenocarcinoma of the pancreas. Eur J Cancer. Aug 2014;50(12):2072–2081. [PubMed: 24915778]
45. Chung V, McDonough S, Philip PA, Cardin D, Wang-Gillam A, Hui L, et al. Effect of Selumetinib and MK-2206 vs Oxaliplatin and Fluorouracil in Patients With Metastatic Pancreatic Cancer After Prior Therapy: SWOG S1115 Study Randomized Clinical Trial. JAMA Oncol. Apr 1 2017;3(4):516–522. [PubMed: 27978579]
46. Lito P, Rosen N, Solit DB. Tumor adaptation and resistance to RAF inhibitors. Nat Med. Nov 2013;19(11):1401–1409.
47. Long GV, Fung C, Menzies AM, Pupo GM, Carlino MS, Hyman J, et al. Increased MAPK reactivation in early resistance to dabrafenib/trametinib combination therapy of BRAF-mutant metastatic melanoma. Nat Commun. Dec 2 2014;5:5694. [PubMed: 25452114]
48. Paraiso KH, Fedorenko IV, Cantini LP, Munko AC, Hall M, Sondak VK, et al. Recovery of phospho-ERK activity allows melanoma cells to escape from BRAF inhibitor therapy. Br J Cancer. Jun 8 2010;102(12):1724–1730. [PubMed: 20531415]
49. Bryant KL, Stalnecker CA, Zeitouni D, Klomp JE, Peng S, Tikunov AP, et al. Combination of ERK and autophagy inhibition as a treatment approach for pancreatic cancer. Nat Med. Apr 2019;25(4):628–640. [PubMed: 30833752]
50. Hayes TK, Neel NF, Hu C, Gautam P, Chenard M, Long B, et al. Long-Term ERK Inhibition in KRAS-Mutant Pancreatic Cancer Is Associated with MYC Degradation and Senescencelike Growth Suppression. Cancer cell. Jan 11 2016;29(1):75–89. [PubMed: 26725216]

Author Manuscript Author Manuscript Author Manuscript Author Manuscript

- Increases in phosphorylated ERK and Drp1 induced by pharmacological ascorbate (P-AscH$^-$) were reversed with genetic and pharmacological inhibitors of ERK and Drp1, as well as in cells lacking functional mitochondria.
- Pharmacological ascorbate increased Drp1 colocalization to mitochondria, decreased mitochondrial volume, increased disconnected components, and decreased mitochondrial length, suggesting an increase in mitochondrial fission after treatment with pharmacological ascorbate.
- Pharmacological ascorbate decreased clonogenic survival which was enhanced by genetic and pharmacological inhibition of both ERK and Drp1. In murine xenografts, the combination of pharmacological ascorbate and pharmacological inhibition of Drp1 increased overall survival.
- These results suggest that pharmacological ascorbate induces sustained increases in mitochondrial oxidative stress and changes in mitochondrial dynamics, through activation of the ERK/Drp1 signaling pathway, an adaptive response.

Author Manuscript Author Manuscript Author Manuscript Author Manuscript

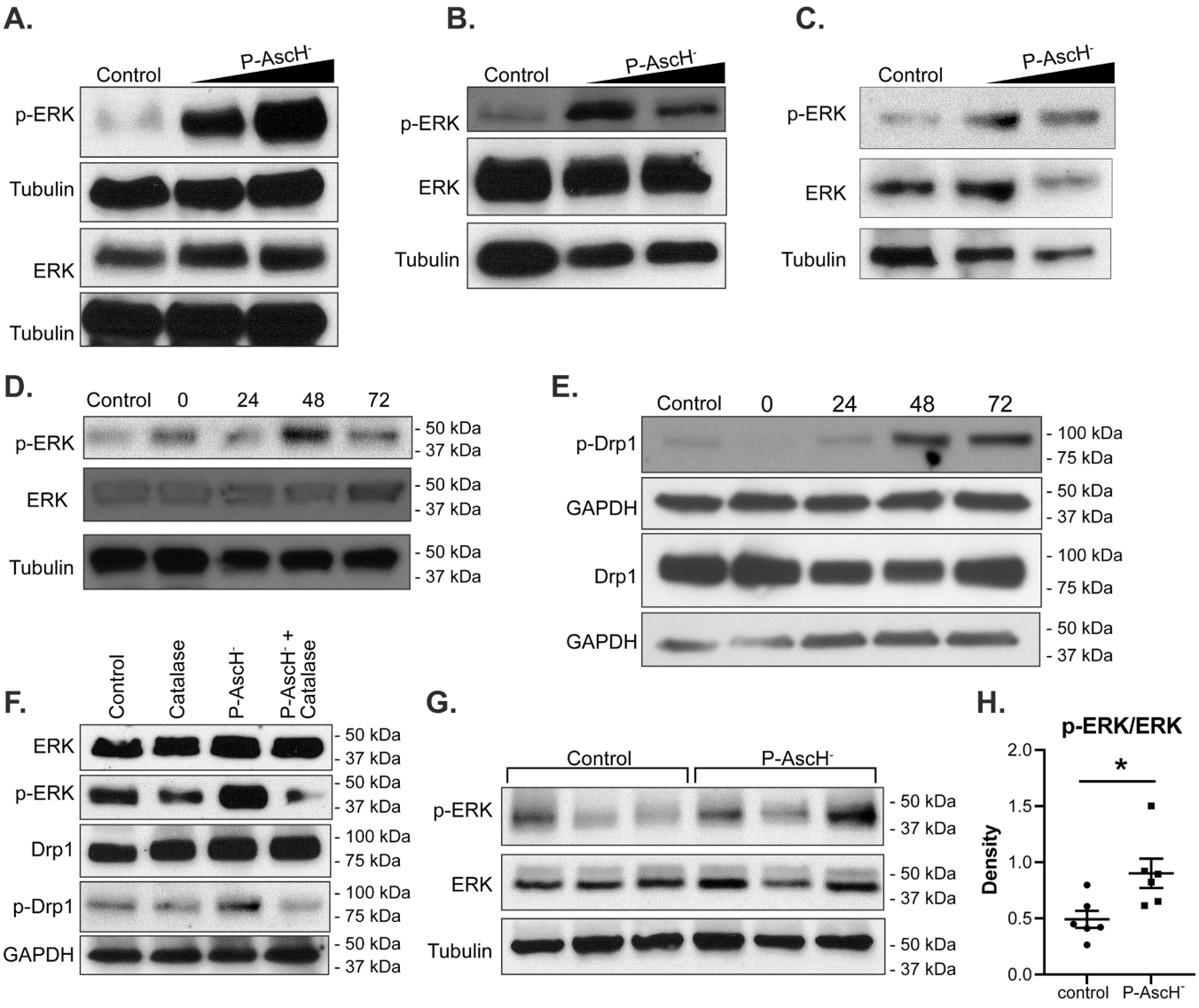

Figure 1. Generation of H_2O_2 by P-AscH$^-$ activates ERK and Drp1.

339, MIA PaCa-2, and H6c7 cells were treated with P-AscH$^-$ (5–30 pmole/cell, 1–2 mM for 1 h). Protein was isolated for Western blot 48 h after treatment.

A. P-AscH$^-$ increases p-ERK in the patient-derived cell line 339.

B. P-AscH$^-$ increases p-ERK in MIA PaCa-2 cell line.

C. P-AscH$^-$ does not alter p-ERK in the non-tumorigenic pancreatic ductal epithelial cell line H6c7.

D. MIA PaCa-2 cells treated with P-AscH$^-$ (10 pmole/cell, 1 mM for 1 h) and protein was isolated at 0, 24, 48, and 72 h after treatment demonstrating increased p-ERK.

E. MIA PaCa-2 cells treated with P-AscH$^-$ (10 pmole/cell, 1 mM for 1 h) increased Drp1 levels at 48 and 72 h.

F. MIA PaCa-2 cells were treated with 100 μg/mL of catalase, P-AscH$^-$ (10 pmole/cell, 1 mM for 1 h), or catalase and P-AscH$^-$. Protein isolated 48 h after treatment for western blotting demonstrates reversal of P-AscH$^-$-induced increased p-ERK and p-Drp1.

Author Manuscript Author Manuscript Author Manuscript Author Manuscript

G. Established MIA PaCa-2 PDAC xenografts were treated with P-AscH$^-$ (4 g/kg, i.p., b.i.d.) or saline b.i.d. for 5 d (n = 6/group). Representative Western blots from harvested tumors.

H. Quantification of western blots of tumor xenografts using densitometry demonstrate increased ratio of p-ERK/ERK in the mice receiving P-AscH$^-$ compared to saline treated mice (*p = 0.02, Student's t-test).

Author Manuscript Author Manuscript Author Manuscript Author Manuscript

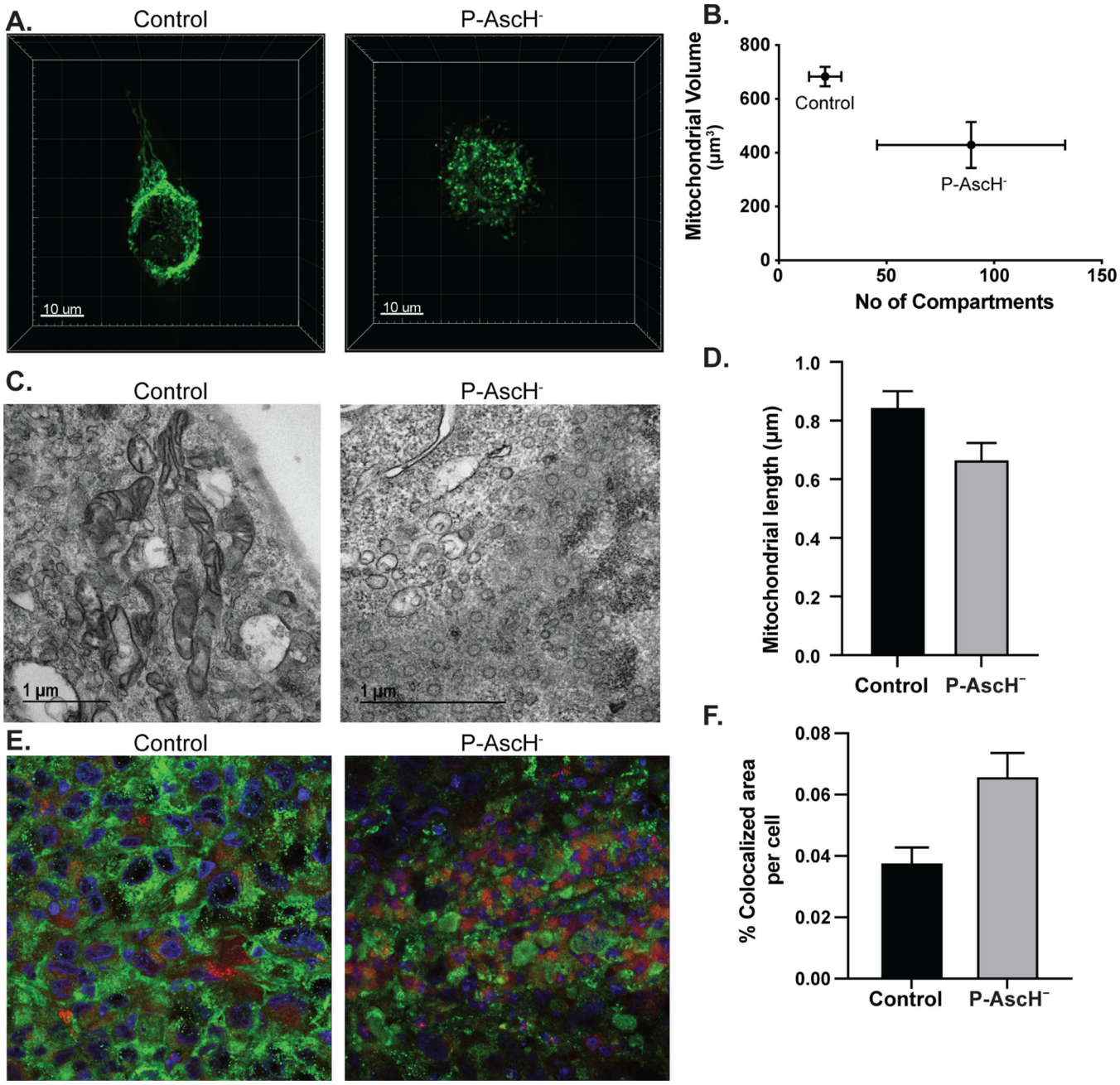

Figure 2. P-AscH^{-} induces mitochondrial fission *via* Drp1 activation in PDAC.

A. Confocal Microscopy for mitochondrial compartments and volume. Representative confocal images of MIA PaCa-2 cells stained with MitoTracker green 48 h after being treated with P-AscH^{-} (10 pmole/cell, 1 mM) for 1 h *vs.* control.

B. Quantification of confocal microscopy for mitochondrial compartments and volume MitoTracker Green immunofluorescence demonstrates increased mitochondrial compartments and decreased total mitochondrial volume consistent with mitochondrial fission.

Author Manuscript Author Manuscript Author Manuscript Author Manuscript

C. Representative images of electron microscopy of MIA PaCa-2 cells 48 h after P-AscH$^-$ treatment.

D. Quantification of electron microscopy demonstrating decreased mitochondrial length in MIA PaCa-2 cells treated with P-AscH$^-$ (*p = 0.02). Mitochondria (control = 545, P-AscH$^-$ = 589) were quantified from images taken from 4 saline treated and 5 P-AscH$^-$ treated cells.

E. Confocal images of a MIA PaCa-2 xenograft. Athymic nude mice, established tumor xenografts were treated with 1.0 M NaCl or P-AscH$^-$ (4 g/kg) twice daily for 5 d. Mitochondrial networks shown green pixels and p-Drp1 bright orange pixels, where yellow pixels indicating p-Drp1 translocated to mitochondria.

F. Quantification of colocalization using ImageJ demonstrates significant increases in colocalization after P-AscH$^-$ treatment. (*p = 0.02 saline *vs.* P-AscH$^-$ treated mice. Data include 8 images from 4 saline treated animals *vs.* 14 images from 5 P-AscH$^-$treated animals.

Author Manuscript Author Manuscript Author Manuscript Author Manuscript

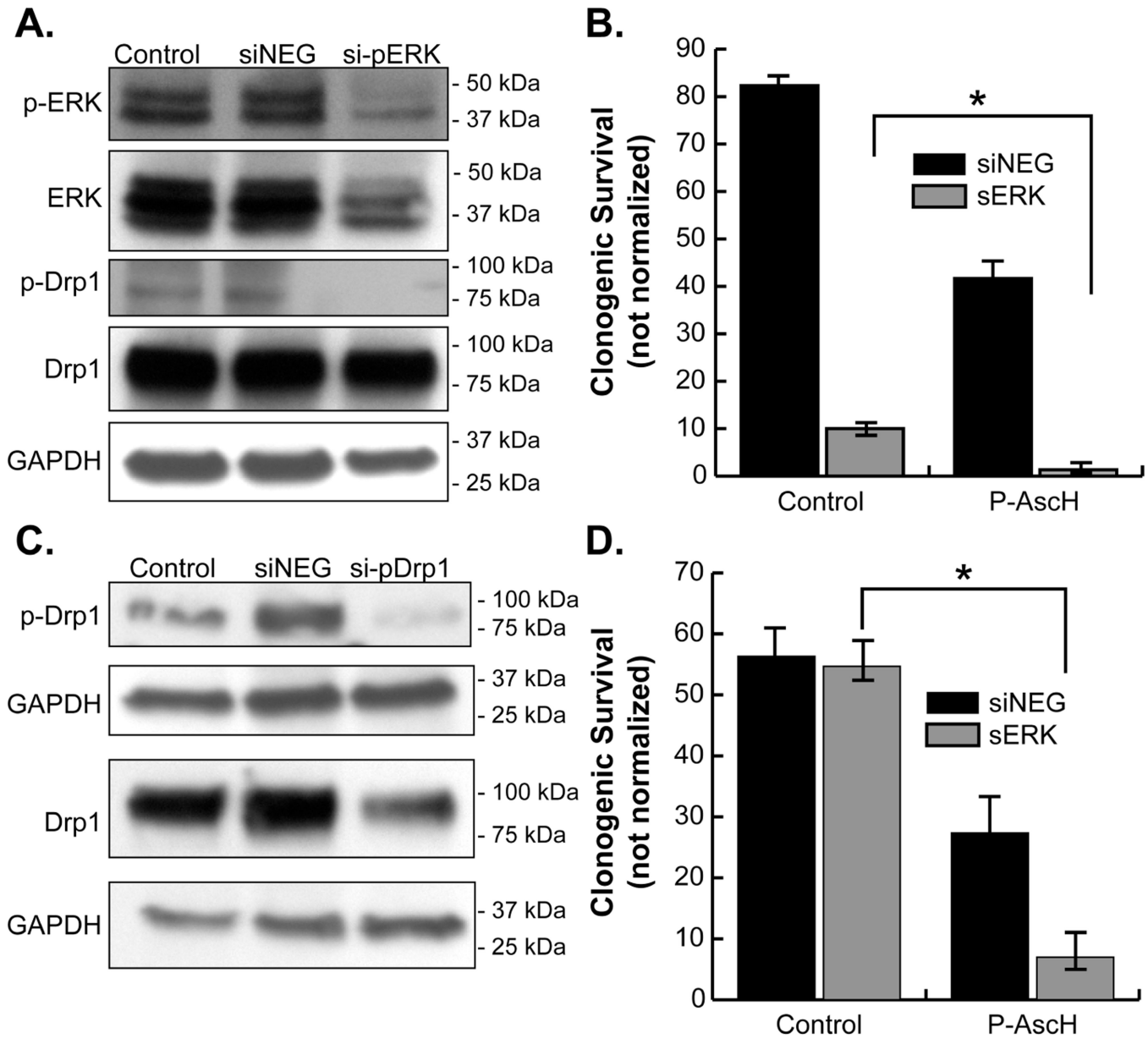

Figure 3. Genetic inhibition of ERK or Drp1 sensitizes cancer cells to P-AscH$^-$.

A. Decreases in immunoreactive protein for p-ERK and p-Drp1 levels in the siERK knockout cells.

B. Clonogenic survival was performed in siERK and siNEG cell lines after treatment with P-AscH$^-$ (7 pmole/cell) for 1 h. Clonogenic survival was decreased in the siERK cells compared to the siNEG cells when treated with P-AscH$^-$ (*$p < 0.01$, Means ± SEM, $n = 3$).

C. Decreases in immunoreactive protein for p-Drp1 in the Drp1 knockout cells.

D. Clonogenic survival assays were performed in the siDrp1 and siNEG cell lines after exposure to P-AscH$^-$ (7 pmole/cell) demonstrate significant decreases in number of colonies in the siDrp1 cells compared to siNEG cells (*$p = 0.02$, Means ± SEM, $n = 3$).

Author Manuscript Author Manuscript Author Manuscript Author Manuscript

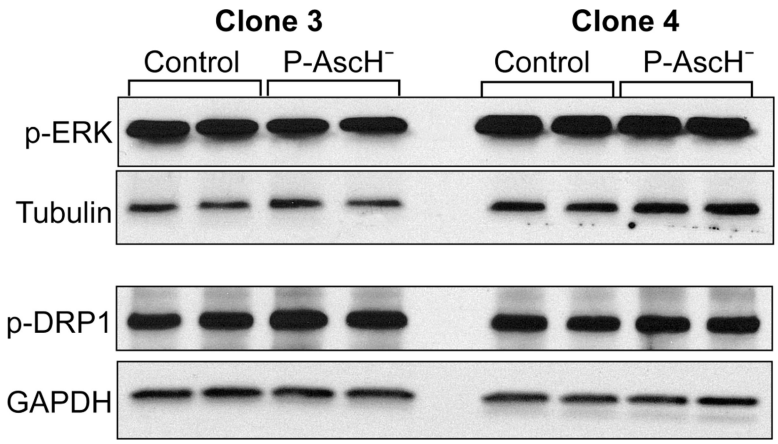

Figure 4. ρ^0 cells demonstrate inhibition of P-AscH$^-$-induced changes in p-ERK and p-Drp1.

ρ^0 cells were treated with 10 pmole/cell (1 mM) P-AscH$^-$ for 1 h and protein was isolated 48 h later. Neither clone 3 nor clone 4 ρ^0 cells demonstrated changes in p-ERK or p-Drp1 immunoreactive protein expression following treatment with P-AscH$^-$ compared to control. Representative blots are shown.

Author Manuscript
Author Manuscript
Author Manuscript
Author Manuscript

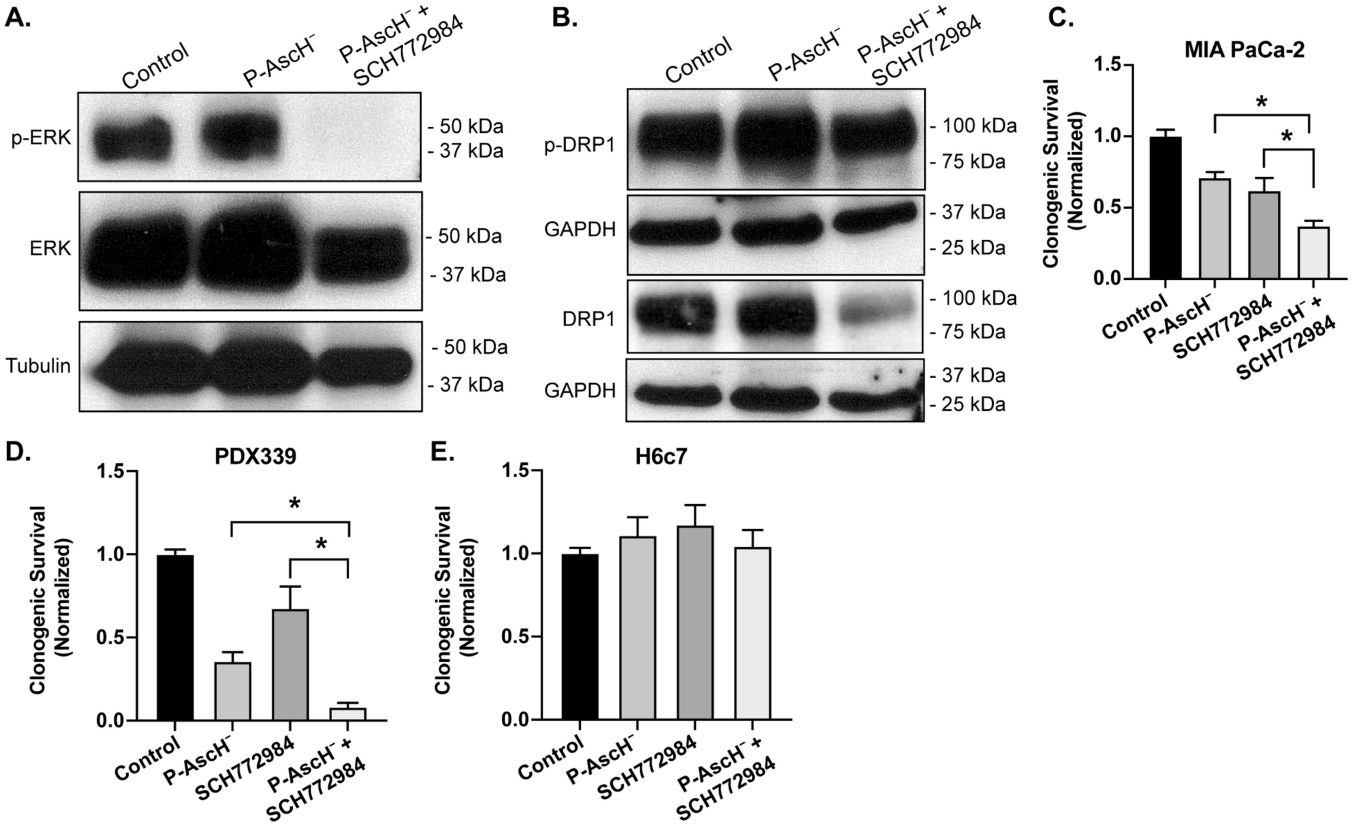

Figure 5. Pharmacological inhibition of ERK sensitizes cancer cells to P-AscH⁻.

MIA PaCa-2 cells were treated with P-AscH⁻ (10 pmole/cell, 1 mM) for 1 h, immediately followed by the ERK inhibitor SCH772984 (500 nM) for 24 h.

A. Western blot analysis 48 h after P-AscH⁻ treatment shows decreased p-ERK1 in cells treated with SCH772984 compared to those treated with P-AscH⁻ alone.

B. Western blot analysis 48 h after P-AscH⁻ treatment shows decreased p-Drp1 in cells treated with SCH772984 compared to those treated with P-AscH⁻ alone.

C. Decreased clonogenic survival in cells treated with P-AscH⁻, SCH772984, or the combination in MIA PaCa-2 cells (*$p < 0.05$, Means ± SEM, $n = 3$).

D. Decreased clonogenic survival in the PDX339 cell line with P-AscH⁻, SCH772984 or the combination (*$p < 0.05$, Means ± SEM, $n = 3$).

E. No changes in clonogenic survival in the non-tumorigenic pancreatic ductal epithelial cell line H6c7 with P-AscH⁻, SCH772984 or the combination.

Author Manuscript Author Manuscript Author Manuscript Author Manuscript

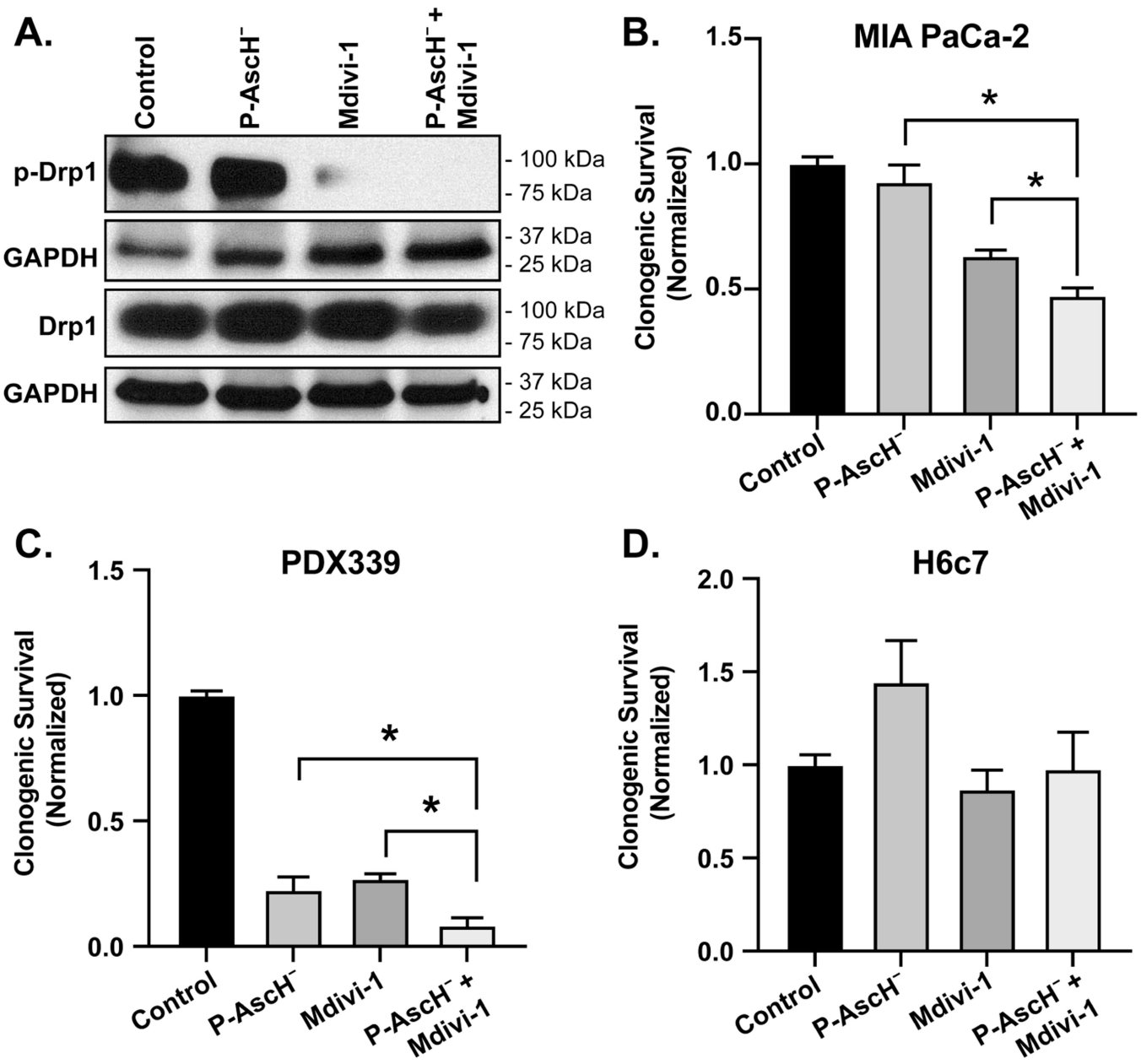

Figure 6: Pharmacological inhibition of Drp1 sensitizes cancer cells to P-AscH⁻.

MIA PaCa-2 cells were treated with P-AscH⁻ (10 pmole/cell, 1 mM) for 1 h, immediately followed by Mdivi-1 (25 μM – 50 μM).

A. Western blot analysis 48 h after P-AscH⁻ treatment show decreased p-Drp1 in cells treated with Mdivi-1compared to those treated with P-AscH⁻ alone.

B. MIA PaCa-2 cells were treated with P-AscH⁻ for 1 h followed by Mdivi-1 (50 μM) for 24 h. Clonogenic survival demonstrated significantly decreased colony formation with the combination treatment compared to either treatment alone in MIA PaCa-2 cells (*$p < 0.01$, Means ± SEM, $n = 3$).

C. PDX339 cells had significantly decreased colony formation when treated with P-AscH⁻ + Mdivi-1 (50 μM) compared to P-AscH⁻ alone (*$p < 0.05$, Means ± SEM, $n = 3$).

Author Manuscript Author Manuscript Author Manuscript Author Manuscript

D. Clonogenic survival in the H6c7 cell line demonstrated no changes in any of the treatments compared to controls ($p > 0.05$, Means ± SEM, $n = 3$).

Author Manuscript Author Manuscript Author Manuscript Author Manuscript

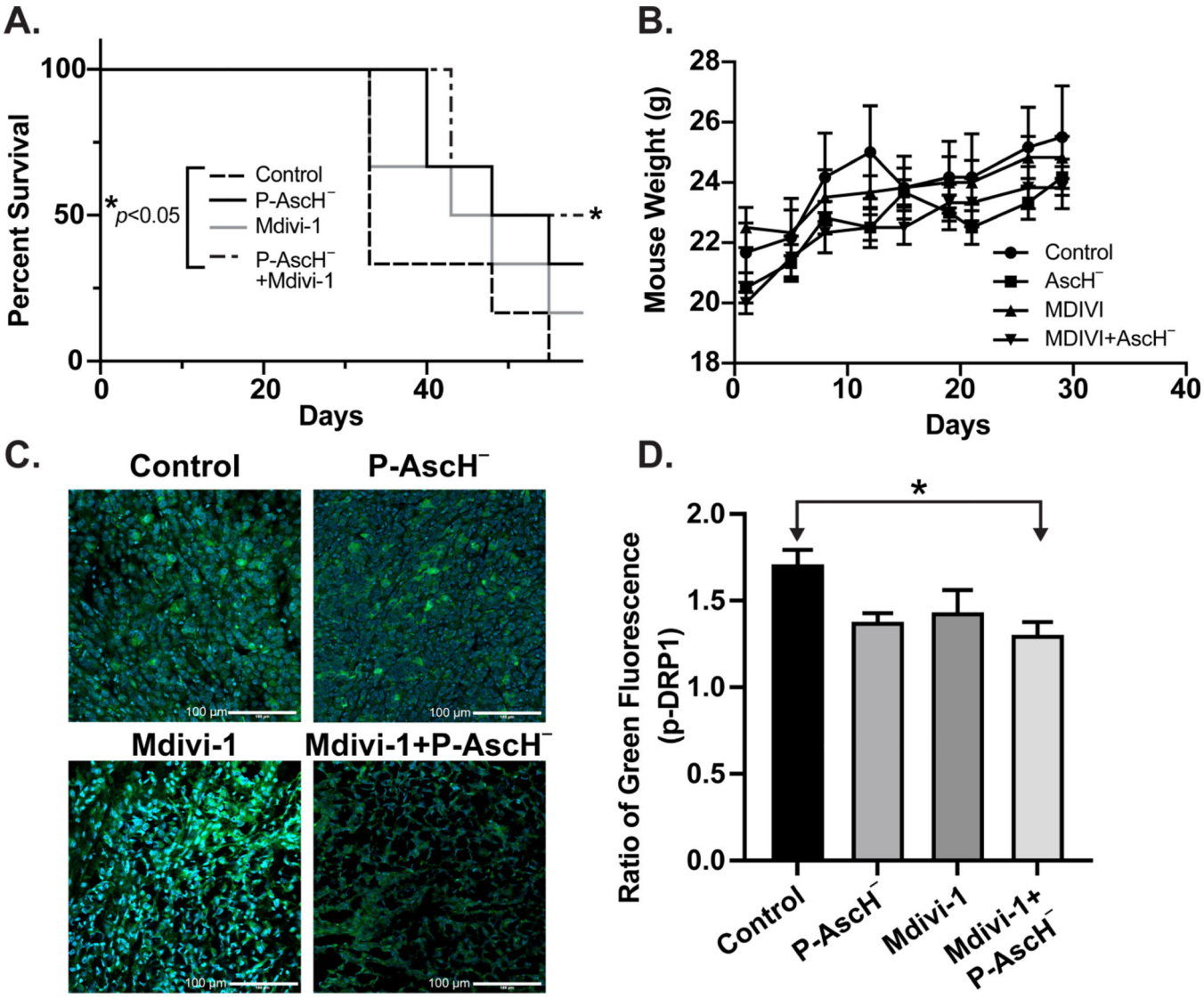

Figure 7: Mdivi-1 plus P-AscH$^-$ increases PDAC survival *in vivo*.

MIA PaCa-2 xenografts were created with flank injections in nude mice. After tumors developed, mice received daily i.p. injections of saline control ($n = 6$), P-AscH$^-$ (4 g/kg, $n = 6$), Mdivi-1 (50 mg/kg, $n = 6$), or both drugs ($n = 6$) for 21 days.

A. Mice treated with both drugs had the greatest increase in median survival compared to control (54.5 *vs.* 33 days, *$p < 0.05$, Log-rank Mantel-Cox test).

B. Drug treatments were well tolerated in all groups with no significant differences in body weights between groups throughout the experiment.

C. Tumor samples were fixed incubated with p-Drp1 antibody and then secondary antibody. DAPI was used to stain the cell nuclei. Representative tumor sections demonstrate decreased p-Drp1 immunofluorescence in xenografts treated with the combination of P-AscH$^-$ + Mdivi-1.

D. Images were quantified using ImageJ. The ratios of green fluorescence p-Drp1 over DAPI (blue) were recorded demonstrating decreased p-Drp1 immunofluorescence in xenografts

Author Manuscript Author Manuscript Author Manuscript Author Manuscript

treated with P-AscH$^-$ and Mdivi-1 (*p = 0.05, Control *vs.* Mdivi-1 + P-AscH$^-$, one way ANOVA Dunnett's multiple comparison test).

Author Manuscript Author Manuscript Author Manuscript Author Manuscript

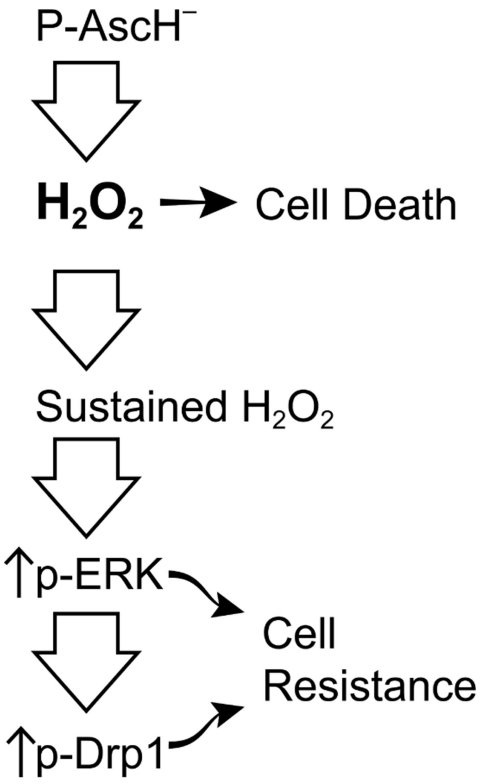

Figure 8. Concepts and results in support of the hypothesis.

While the initial increased generation of H_2O_2 is toxic to PDAC cells, sustained generation of H_2O_2 subsequently leads to resistance *via* late activation of the ERK pathway. Inhibiting this pathway with either ERK or p-Drp-1 inhibitors may prove beneficial in overcoming resistance to P-AscH^-.